

## DEVELOPMENT OF AN EMBEDDED FPGA-BASED DATA ACQUISITION SYSTEM DEDICATED TO ZERO POWER REACTOR NOISE EXPERIMENTS

Mohammad Arkani<sup>1,2)</sup>, Hossein Khalafi<sup>2)</sup>, Naser Vosoughi<sup>3)</sup>

1) Physics Department, Amir-Kabir University of Technology, Hafez Avenue Tehran, Iran (markani@aeoi.org.ir).

2) Radiation Application Research School, Nuclear Science & Technology Research Institute (NSRTI) Atomic Energy Organization of Iran, Tehran, Iran (✉ hkhalfi@aeoi.org.ir).

3) Department of Energy Engineering, Sharif University of Technology, Azadi Street, Tehran, Iran (nvosoughi@sharif.ir).

### Abstract

An embedded time interval data acquisition system (DAS) is developed for zero power reactor (ZPR) noise experiments. The system is capable of measuring the correlation or probability distribution of a random process. The design is totally implemented on a single Field Programmable Gate Array (FPGA). The architecture is tested on different FPGA platforms with different speed grades and hardware resources. Generic experimental values for time resolution and inter-event dead time of the system are 2.22 ns and 6.67 ns respectively. The DAS can record around 48-bit  $\times$  790 kS/s utilizing its built-in fast memory. The system can measure very long time intervals due to its 48-bit timing structure design. As the architecture can work on a typical FPGA, this is a low cost experimental tool and needs little time to be established. In addition, revisions are easily possible through its reprogramming capability. The performance of the system is checked and verified experimentally.

Keywords: zero power reactor (ZPR) noise; time interval measurement; probability distribution function (PDF); field programmable gate array (FPGA); data acquisition system (DAS); nuclear reactor, neutron detection.

© 2014 Polish Academy of Sciences. All rights reserved

### Nomenclature

$C_i$ : Number of digitization periods counted by the counter.

$^{60}\text{Co}$ : Cobalt-60 radioisotope which is a radioactive gamma source.

DAS: Data acquisition system.

DDS: Direct digital synthesizer.

DMA: Direct memory access.

FIFO memory: First-in first-out memory.

FPGA: Field programmable gate array.

G-M: Geiger-Muller.

IDE: Integrated development environment.

JE: Jitter error.

N: Number of digitization periods between two successive input pulses.

NIM: Nuclear instrumentation module.

PCB: Printed circuit board.

PDF: Probability distribution function.

PLL: Phased locked loop.

PSD: Power spectral density.

P/s: Pulse per second.

SDRAM: Synchronous dynamic random access memory.

S/s: Samples per second.

T: Digitization period.

TDC: Time to digital converter.

TIME: Time interval measurement error.

TRR: Tehran Research Reactor.

USB: Universal serial bus.

ZPR: Zero power reactor.

$\Delta$ : Analyzer sweep.

$\Delta_i$ : Time interval.

## 1. Introduction

### 1.1. ZPR noise

One of useful diagnostic methods of nuclear reactors is ZPR noise analysis. The novel idea is to measure the statistical information of random fluctuations of neutron density in the reactor core and relating the experimental results to the background theory [1–4]. Reactor noise experiments have great advantages in reactor analysis as follows: the method is low-cost, no perturbation in experimental case study is needed, and measurement is possible during operation. Moreover, its uniqueness in measuring some important parameters such as sub-criticality measurement, absolute effective delayed neutron fraction measurement, and prompt neutron lifetime in multiplying media are other advantages of the method.

Four common ZPR noise experiments are Rossi- $\alpha$  (Type-I and Type-II), Feynman- $\alpha$ , and power spectral density (a frequency domain analysis method). Since required data analyses of these experiments on fluctuations of neutron density are different, traditionally, their experimental instruments are also different. Fig. 1-a shows Rossi- $\alpha$  type-I analysis (Rossi- $\alpha$  is a time domain reactor noise experiment). This method measures the probability of  $e^{-\alpha t} dt$  at a time  $t$  following a count at  $t=0$ . Every count is a triggering event (determining the time origin). Orndroff [5] has designed a time analyzing system for Rossi- $\alpha$  type-I experiment. This system measures the time intervals of the pulses with a time resolution of 250 ns. This is accomplished by using a ten-channel time analyzer with delay lines between channels. The Rossi- $\alpha$  type-II method is illustrated in Fig. 1-b. The analyzer is ready to be triggered and starts waiting for the first count. When the triggering count arrives, the analyzer starts to record the time interval of the pulses. It is assumed that the analyzer sweep (abbreviated as  $\Delta$  in Fig. 1-b) is long enough to include all the counts from a neutron chain. In an alternative analysis of the data, pulses are counted in different time windows and then are evaluated to find the variance to mean ratio of the gathered information. This method is known as Feynman- $\alpha$  or variance-to-mean ratio. Reactivity, prompt neutron life time, and effective delayed neutron fraction can be estimated by curve fitting of the reactor noise theoretical expressions to the experimental data.

In frequency domain experiments, a current type neutron detector is usually employed. PSD which is defined as Fourier transform of the auto correlation function is measured by using analog signal processing circuits [6]. An ion chamber is biased in the current mode. Frequency of interest of the output current is selected by a band pass filter. Then, the power of the signal is measured which gives the power at the frequency. There are some efforts to do the PSD measurements using the pulse mode neutron detection equipment [6, 7]. The main advantage of this technique is the elimination of some electronic modules which are needed in the current mode experiments. Moreover, any electronic system has multiple sources of electrical noise in the form of random voltage or current waveform, both “internal” and “external”. “Internal” (or intrinsic) sources that are parts of the circuit itself; resistors, amplifiers, transistors, etc. “External” refers to the noise present in the signal being applied to the circuit or to noise introduced into the circuit by another means, such as conducted on a system ground or received on one of the many antennas formed by the traces and components

in the system. Because of the way that the information is encoded in analog circuits, they are much more susceptible to noise than digital circuits. A small change in the signal can represent a significant change in the information, which can cause the information to be lost. Since digital signals take on one of only two different values, a disturbance would have to be about one-half of the magnitude or voltage level standard of the digital signal to cause an error; this property of digital circuits can be exploited to make signal processing noise-resistant. In digital electronics, because the information is quantized, as long as the signal stays inside a range of values, it represents the same information. Digital circuits use this principle to regenerate the signal at each logic gate, lessening or removing noise. Therefore, more accurate measurements can be carried out based on pulse mode neutron detection. Frequency bandwidth of analog modules is limited. Cabling and impedance matching in transmission of the signals in the electronic chain causes signal attenuation. Therefore, the PSD measured in an current mode experiment is distorted. In the pulse mode experiment, the same signal attenuation between neutron detector and electronic circuits occurs. Therefore, pulse height information is lost. As reactor noise experiments need time information of the pulses, the time information in pulse mode operation is easily preserved

Traditionally, each reactor noise experiment has its own especial hardware design for data analysis. Kitamura [7] has performed reactor noise experiments by using a computer based DAS. The equipment acquires experimental data of the pulses. The analysis of the data was performed based on software programming. No evaluations on TIME and stability of the DAS were performed by the authors. In addition, the practical time resolution and inter-event dead time of the system are reported equal to 1  $\mu$ s and 100ns respectively. For fast critical systems, better timing features of an appropriate ZPR noise DAS are required. High performance TDCs based on state-of-the art technology are investigated in the literature [8-11]. Therefore, this research work was aimed to develop a dedicated ZPR noise DAS based on modern digital

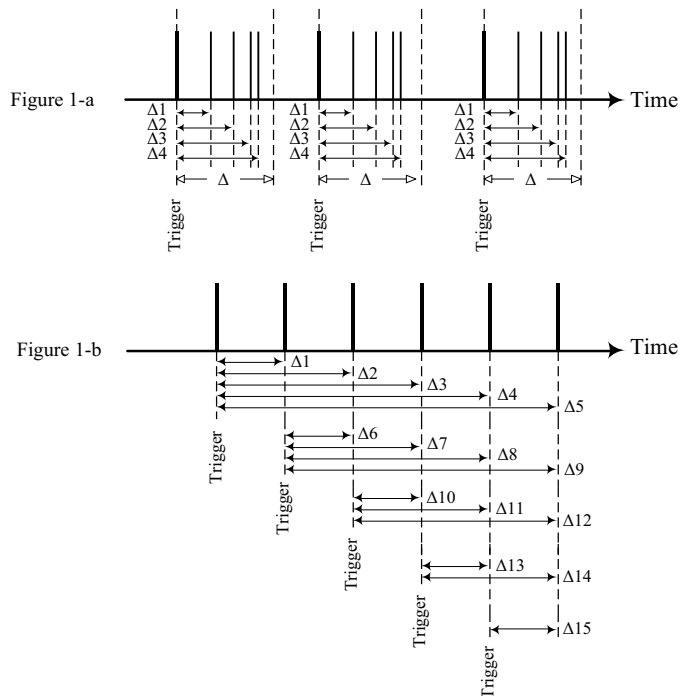


Fig. 1. Methods of Rossi- $\alpha$  data analysis (a. Rossi- $\alpha$  Type-I, b. Rossi- $\alpha$  Type-II).

electronic technology. With the equipment, future research in depth into the applications and development of ZPR noise theory is possible.

### 1.2. Time interval measurement

In the previous section, methods of reactor noise analysis were explained. As arbitrary data analysis is applied to the experimental data, error accumulation might be a significant problem. Each time interval, measured by the experimental tool has its own TIME. Therefore, analysis of few random time intervals ( $\Delta 1$  to  $\Delta 5$  in Figure 1-b as an example), has an accumulated TIME which is the summation of all uncertainties. This is clearly seen in Fig. 2. The time interval error is the summation of the systematic error (the digitization period), and the JE of the clock oscillator. If the arrival times of the pulses are recorded, the systematic error can be reduced to one digitization period for any arbitrary analysis of the data. This is shown in Fig. 3, which is the basis of the ZPR noise DAS presented in this paper. By this method, the number of numerical operations for time interval calculation is limited to one subtraction between two arrival times. While by the method shown in Fig. 2, as the recorded data is the differential time between successive random pulses, the time interval is the summation over many subtractions. Therefore, the error is increased due to the multiple numerical operations.

The method shown in Fig. 3 is applied to the present work to record the arrival times of the random pulses. As data of the random process is measured by the equipment, all required signal processing and operations can be performed by powerful engineering tools like MATLAB software [12]. Various methods of mathematical data analysis are possible by software programming instead of hardware-based signal processing.

As a brief review of important parameters of time interval measuring systems, they can be listed as long interval measurement range, linearity, low measurement uncertainty or little standard deviation, short inter-event dead time, high sampling rate, and high resolution or small digitization period. Kalisz [13] and Zieliński [14] have explained a detailed description of these parameters. In addition, useful books on design, modeling and testing of TDCs are published [15, 16].

As time intervals between neutron detection events are random, the measuring system must be fast enough to minimize the loss of experimental data. Therefore, inter-event dead time is expected which must be lowered to be as short as possible. In addition, saving data on the memory and data transfer should be accomplished in parallel.

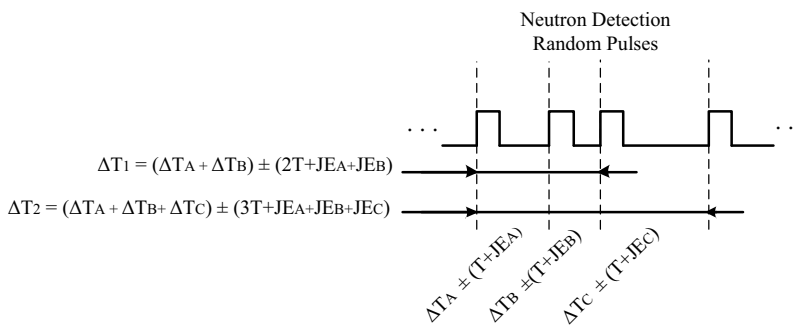


Fig. 2. Arbitrary analysis and error accumulation of the data in TDCs which measure time intervals of consecutive random pulses.

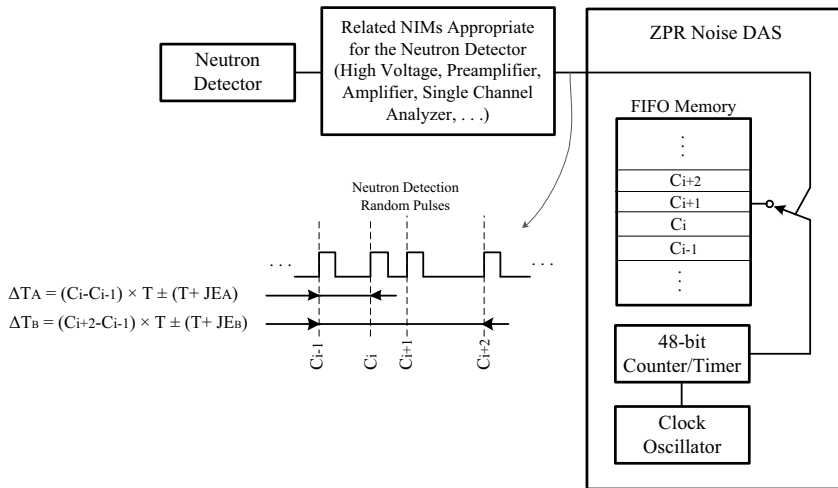


Fig. 3. General principle of the present ZPR noise DAS. As arrival times of the pulses are recorded, systematic error is limited to  $\pm T$  in any arbitrary analysis of the data.

## 2. Embedded system architecture

Figure 4 shows the general schematic diagram of the system architecture. An external crystal oscillator is the basis for time discretization. The frequency is scaled by the PLL block implemented in the device in order to achieve the best possible speed performance. Note that due to compactness of the internal circuits of the device, the maximum internal working frequency is higher than the maximum pin communication frequency. All parts of the design are synchronized with the clocks provided by the PLL. A NIOS II embedded processor [17] works at a different frequency (refer to Table 1), the PLL block also generates the appropriate clock for this part.

The 48-bit counter block counts the time based on the FPGA global clock. Due to the 48-bit timing structure, the time interval measuring range of the system is very long<sup>1</sup>. Detected events are fed into the FPGA through an input channel at the level of LVTTTL standard through an SMA connector. The writing control logic of FIFO memory is sensitive to the rising edges of the input pulses to register the time counted by the counter, into the FIFO memory block. At least three digitization periods are needed to finalize each sampling process of the input pulses. Therefore, the minimum inter-event dead time of the system is equal to  $3 \times T$ . The inter-event dead time of the system was examined experimentally using a high frequency pulse train test signal (based on hardware platform B). As a result, the FIFO memory overflow after 512 samples (refer to Table 1 to find the maximum sampling rate parameter and FIFO memory depth of the hardware). Below 100 MHz ( $>10$ ns time interval), the system has recorded 512 time intervals, and then FIFO memory overflow. Above this, 512 samples were recorded incorrectly. Then, overflow of the memory occurred. Therefore, the dead time of the system is 10ns as it is expected based on the implemented logic for data sampling.

1- Cycle time of the 48-bit timer/counter =  $\frac{2^{48} \times T}{3600 \times 24} \Big|_{T=2.2\text{ns}} \approx 7.17 \text{ day}$

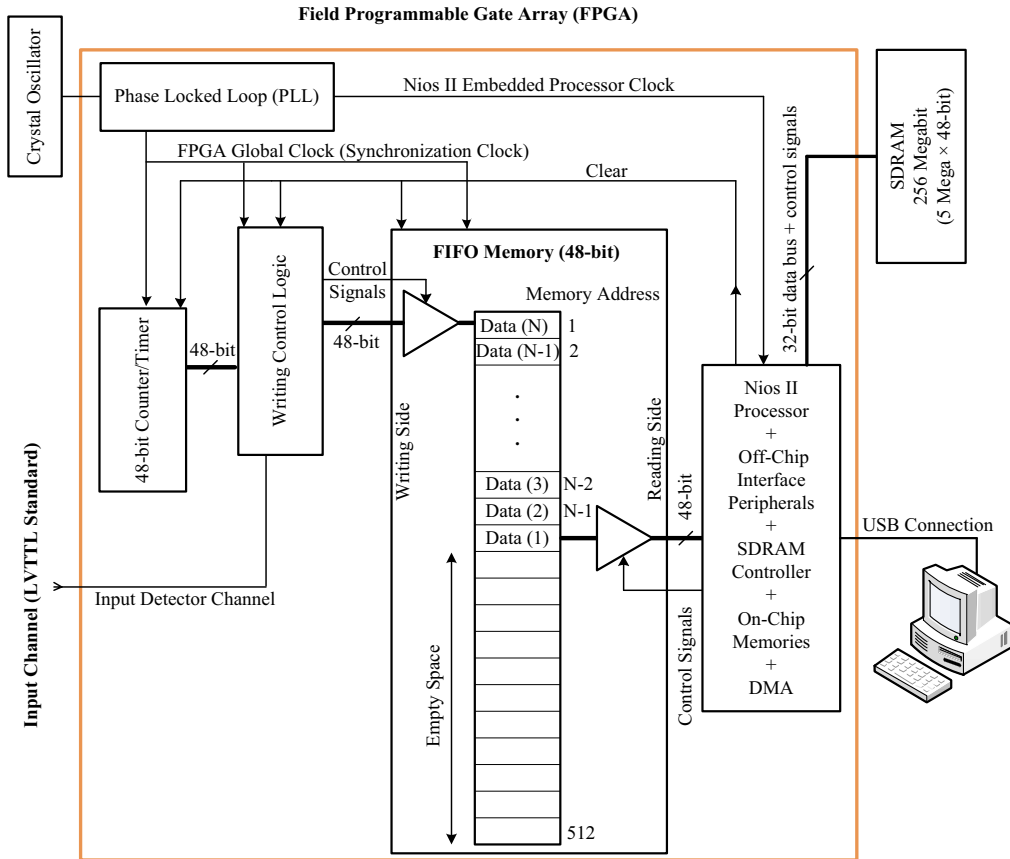


Fig. 4. General schematic diagram of the ZPR noise DAS.

Since communication with the computer is comparatively slow, the stored data in the FIFO memory is transferred to the SDRAM memory by the NIOS II embedded processor temporarily. Finally, the computer fetches the data through the USB connection. Actually, the maximum speed of data transfer is limited by the computer port.

### 2.1. Influence of clock instability on TIME

The precision of time interval measurement is determined by the standard clock signal. Standard clock phase fluctuations and long-term frequency instability depend on the type of oscillator and the environmental factors such as: temperature, vibration, supply voltage fluctuation, and noise [18, 19]. In the special case of the equipment described in this paper, as long interval random pulses may be examined, long term accumulated JE should be taken into account. Long term accumulated jitter is shown in Fig. 5. The time interval between the initial and  $N_{th}$  transition of the oscillator can be treated as a random variable which can be written as equation 1. The first term,  $NT$ , is the average of the time interval measurements. The TIME is a multiplication of the digitization period. The major part of jitter error in oscillators is a random Gaussian function. The coefficient  $k$  is determined by equation 2. For short interval pulses,  $k$  is equal to unity, while for long intervals, as accumulated jitter error of the signal

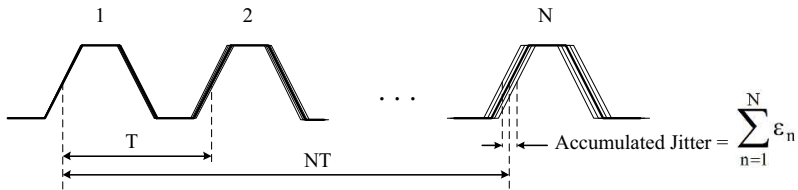


Fig. 5. Accumulated jitter error in N consecutive pulses.

clock increases, higher values of k cause larger TIME. Experimental information on TIME is described in section 3.1 for different constant frequencies of input pulses.

$$\Delta T = NT \pm (k + 1)T, \tag{1}$$

$$k = \text{Round to Nearest Integer Number} \left| \frac{\sum_{n=1}^N \epsilon_n}{T} \right|. \tag{2}$$

## 2.2. System hardware

The structure discussed in previous section can be implemented in any hardware including enough hardware resources. In this work, two hardware platforms are tested for implementation of the system. The first one, Platform-A, is an Altera DSP Development board [20]. Platform-B has been designed and constructed by the authors. This hardware is based on Cyclone III FPGA device family. Future research on applications of ZPR noise theory in TRR will be carried out by this hardware.

Table 1 compares the two types of FPGAs, their embedded resources, and the amounts of elements needed for the embedded system architecture. The first one, Platform-A, shows better performance especially in its speed characteristics. The maximum sampling rate of Platform-B, the hardware with a low speed grade and low cost FPGA device, is 520 kS/s, which is enough for the practical rate range of an ordinary neutron detector.

## 2.3. Embedded system firmware

The firmware of the system is comprised of IP cores, VHDL programming, and a soft processing core. Wide varieties of configurable IP cores of different sizes and complexities optimized for FPGAs have been provided [21]. They are optimized for the specific applications; therefore using the available IP cores can make the design more efficient. The NIOS II is a soft processing core, which is constructed by the hardware resources of the device. An economic CPU type is chosen in the SOPC builder environment [22]. The on-chip driver program of the processor is developed by C programming using Eclipse IDE [17]. Depending on the soft core features, Eclipse IDE builds useful drivers automatically applicable for firmware programming of the embedded processing core. Reduced\_device\_drivers and small\_c\_library check boxes are enabled and c\_plus\_plus check box is disabled in BSP editor of Eclipse IDE due to limited amount of on-chip memory of the device. Other settings are left unchanged as software defaults. FIFO memory is created using

Table 1. Experimental test results for two different hardware platforms.

Hardware Platform	Platform-A STRATIX III EP3SL150F1152C2N	Platform-B CYCLONE III EP3C25Q240C8N
Logic Elements Total (%Used)	113600 (%2)	24624 (%10)
FPGA Memory Bits Total (%Used)	5630976 (%8)	608256 (%73)
PLLs Total / Used	8/1	4/1
48-bit FIFO memory Depth	512×48-bit	512×48-bit
Maximum Digitization Frequency (Minimum Digitization Period)	450 MHz (2.22ns)	300 MHz (3.33ns)
Minimum Inter-event Dead Time <sup>a</sup>	6.67ns	10ns
Maximum NIOS II Working Frequency (Maximum Sampling Rate)	150 MHz (48-bit × 790 kS/s)	100 MHz (48-bit × 520 kS/s)
Maximum Sampling Rate <sup>b</sup>	48-bit × 790 kS/s	48-bit × 520 kS/s
Cost	Relatively High	Low

a. At least three digitization periods are needed to finalize each sampling process.

b. A DDS pulse generator is used for generation of a constant frequency test signal. The frequency, at which the FIFO Full flag was asserted, was recorded as “Maximum Sampling Rate” parameter of the system.

Mega Wizard Plug-In Manager of QUARTUS II software. Using this wizard, the FIFO memory is defined as a single clock normal output mode operation FIFO that is optimized for the best speed features. As writing and reading sides work with the same clock, a single clock FIFO is employed.

### 3. Experimental verifications and results

In order to assure reliable functionality of the DAS, experimental verification tests are necessary. The tests are divided into two types: constant and random time intervals.

#### 3.1. Constant time interval

An appropriate test is measurement of a constant time interval. This test can clarify the measurement uncertainty of the measuring tool and the maximum sampling rate of the system. The maximum sampling rate of the system was determined using a constant time interval pulse train generated by a DDS pulse generator. The results are reported in Table 1 for both platforms.

To have an estimation of TIME of the system, measurements were performed with an independent crystal oscillator of the same type and frequency with the system clock oscillator using FPGA Platform-B. Table 2 shows the experimental results on standard deviation of the measured time intervals. For each frequency, 1200 samples were acquired by the system. The tests are performed at a frequency of 100 MHz. To make a test signal with different frequencies, LPM\_COUNTER IP core is employed in modulus configuration with different count modulus numbers (the column entitled as “Scalar” in Table 2). As both oscillators are

of the same type and frequency<sup>2</sup>, the TIME of the DAS might be defined in terms of standard deviation using equation 3 [18].

$$\sigma_A = \sigma_B \quad \Rightarrow \quad \sigma_A = \frac{\sigma_{A+B}}{\sqrt{2}}, \quad (3)$$

$\sigma_A$  and  $\sigma_B$  refer to the standard deviations of the DAS global clock and the test signal respectively. As the oscillators are of the same type and frequency, it is expected that their standard deviations are also the same.  $\sigma_{A+B}$  is the standard deviation obtained during the measuring process of the constant time interval test signal. At long intervals, one-second time interval, the uncertainty increases up to  $\pm 5.11T$ . This error depends on oscillators utilized by the hardware; using oscillator components with higher accuracy can reduce the uncertainty of the measurements.

A long term stability check of the system is important, to know about the overall accuracy of the system. Figure 6 shows measuring results of the system during 20 minutes of continuous measurement of a constant one-second time interval test signal. Note that the vertical axis is the subtraction of N and  $10^8$  to make the fluctuations more clarified. The results are bounded within  $\pm 12 T$ .

Table 2. Standard deviation of the system at different constant time intervals using two independent and same types, 100 MHz crystal oscillators.

Scalar	Test Signal Frequency [Hz]	Time Interval [ $\mu$ s]	$\frac{\sigma_A}{T}$ , T=10ns
$10^8$	1	$10^6$	5.11
$25 \times 10^6$	4	$25 \times 10^4$	0.792
$4 \times 10^6$	25	$4 \times 10^4$	0.299
$10^6$	$10^2$	$10^4$	0.218
$10^4$	$10^4$	$10^2$	0.074

<sup>2</sup> SUNNY SCO-020 100.000000MHz

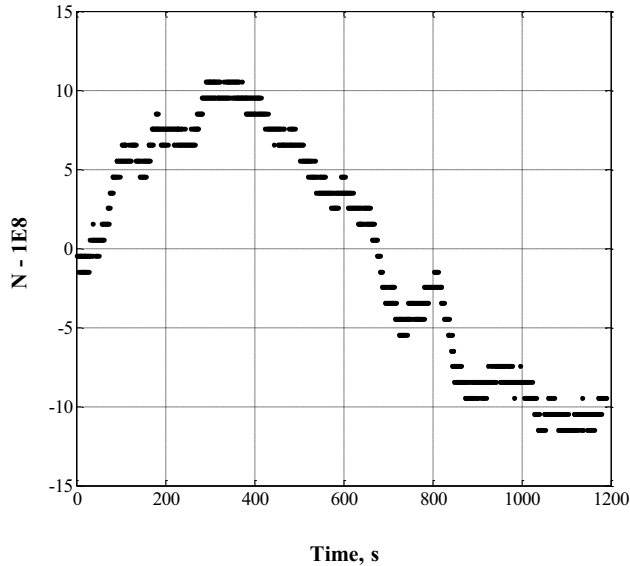


Fig. 6. Long term stability check of the DAS. 20 minutes (=1200 seconds) continuous measurement of one-second time interval test signal.

### 3.2. *Random time interval*

The followings explain the test results on the Platform-A FPGA hardware. Since the principle of ZPR noise experiments is a stochastic phenomenon, the system should be verified by a random pulse train with a known probability distribution. This is performed by using a digital pseudorandom pulse generator. The random time interval generation is based on the inverse transformation method. The random pulse generator was adjusted for Poisson PDF at the pulse generation rate of 500 kP/s. A detailed description of the pulse generator is published in the literature [23]. Figure 7 shows the experimental results. Fig. 7-a shows the random time intervals for  $10^4$  samples. As it is obvious, short interval pulses are more probable. Fig. 7-b shows the time spectrum of the measuring results.

A similar test is possible using a long-lived radioactive source. True Poisson probability distribution of random pulses distorted by the detector dead time is expected. The radioactive Gamma source is a  $^{60}\text{Co}$  radioisotope. The detector is a large G-M tube (ZP1210). Build-up of the positive ion space charges after each discharge process turns the G-M tube off for a specific period of time. A relatively large amount of time should elapse before the next avalanche can take place in the tube. Depending on the physical characteristics of the detector, this time is of the order of 20 to 300  $\mu\text{s}$ . This dead period makes the G-M tube response a nonlinear and complicated function of the incident radiation intensity. Another effect of the detector dead time is the distortion on the time spectrum of the measurements. A detailed description about G-M detectors is available in the literature [24-26]. Figure 8 shows the experimental setup of a ZP1210 G-M detector, which is placed in front of the gamma source. Pulses are amplified and are buffered in the detector housing to minimize the stray capacitance effects. Then, the pulses are passed through a band pass filter and are discriminated from background noise. Finally, they are inverted into 3.3 LVTTTL standard logic level appropriate for the DAS input channel. The test results are shown in Fig. 9. Below 200  $\mu\text{s}$ , distortion of the spectrum is seen due to the dead time effect of the detector. Below 60

$\mu\text{s}$ , there are no recorded events as apparent in Fig. 9-a. Fig. 9-b shows the time spectrum of the pulses.

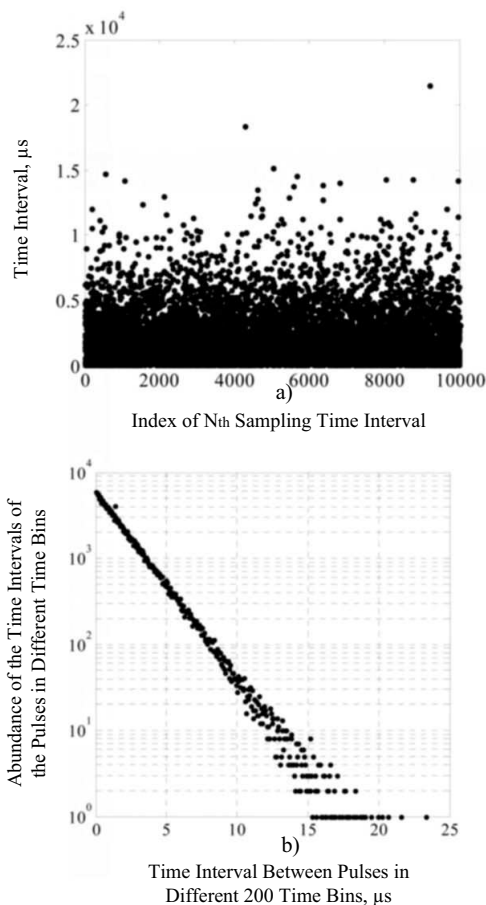


Fig. 7. Measuring results of pseudorandom Poisson pulses (a) Time intervals of  $10^4$  samples, b) The time spectrum of results. (Average Time Interval =  $2.010 \mu\text{s}$ , Number of Analyzed Pulses =  $2.5 \times 10^5$ , Number of Time Bins = 200).

#### 4. Conclusion

The proposed ZPR noise measuring equipment is designed and constructed based on state-of-art technology which offers a modern measuring tool to the scientists in the field of nuclear reactor analysis. The capabilities help the future research in depth to develop the methods, comparative studies, and safety evaluations of nuclear reactors. By recording the arrival times of the pulses, the error in arbitrary analysis of the data is reduced significantly as it was discussed in section 1.2 of the paper (Figs. 2 and 3). The influence of the oscillator clock instability on the TIME of the DAS was examined experimentally in sections 2.1 and 3.1 of the paper; the results are reflected in Table 2 and in Fig. 6. The standard deviation of the results based on one-second time interval test signal (with the features described in section 3.1) is 5.11 T.

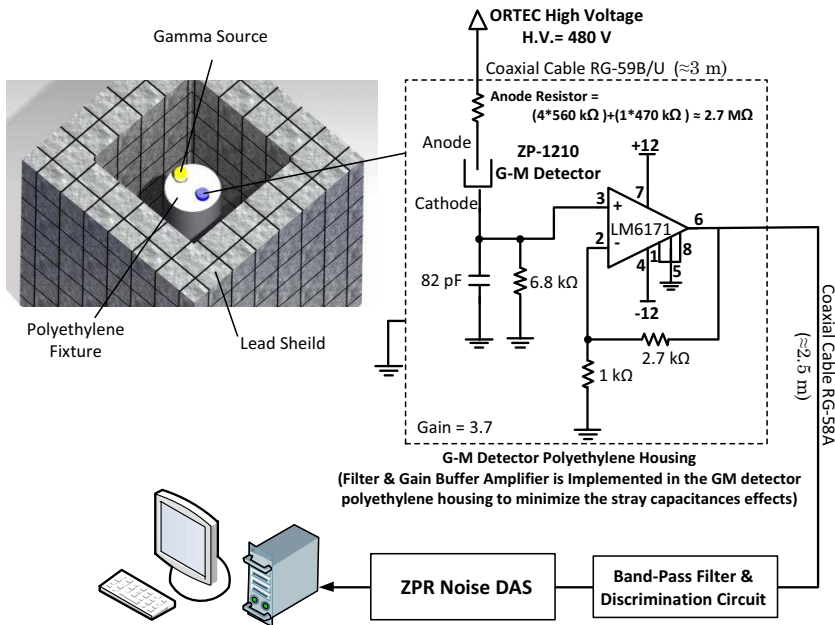


Fig. 8. Experimental set up of ZP1210 G-M detector.

The system is low cost, reprogrammable, easy to upgrade, and easily adaptable to any especial experimental case study.

This equipment has a suitable design for ZPR noise experiments as:

- Short inter-event dead time ( $3 \times T = 6.66 \text{ ns}$ )
- Good resolution in time ( $T = 2.22 \text{ ns}$ )
- High performance in sampling rate and data accumulation of the random pulses. (48-bit  $\times$  790 kS/s)
- Measurement of long time intervals ( $\approx 7.17$  days at  $T = 2.2 \text{ ns}$ )
- Maximum absolute error of  $\pm 12 T$  for one-second time interval pulses (based on experimental results measured by FPGA Platform-B).

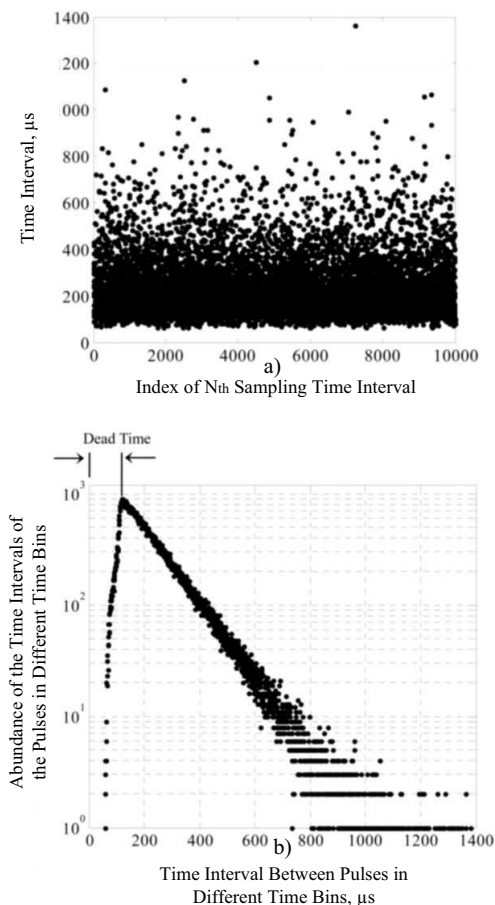


Fig. 9. Time interval distribution of neighboring pulses of a large GM tube (a) Time intervals of  $10^4$  samples, b) The time spectrum of the results (Average Pulse Interval=  $231.012 \mu\text{s}$ , Number of Analyzed Pulses= $2 \times 10^5$ , Number of Time Bins=2000)).

## References

- [1] Thie, J.A., (1963). *Reactor Noise*, Rowman and Littlefield Inc., New York.
- [2] Thie, J.A., (1981). *Power Reactor Noise*, American Nuclear Society, Illinois.
- [3] Uhrig, R.E., (1970). *Random Noise Techniques in Nuclear Reactor Systems*, The Ronald Press Company, New York.
- [4] Williams, M.M.R., (1974). *Random Process in Nuclear Reactors*, Pergamon Press.
- [5] Orndroff, J.D., (1957). *Prompt Neutron Periods of Metal Critical Assemblies*, Nucl. Sci. Eng, 2:450-460.
- [6] Kuramoto, R.Y.R., Santos, A.D., Jerez, R., Diniz, R., (2007). Kinetic Parameters Determination through Power Spectral Densities Measurements using Pulse-Type Detectors in the IPEN/MB-01 Research Reactor, *International Nuclear Atlantic Conference, Santos (Brazil)*.
- [7] Kitamura, Y., Matoba, M., Misavita, T., Unesaki, H., Shiroya, S., (1999). Reactor Noise Experiments by using Acquisition System for Time Series Data of Pulse Train, *J. Nucl. Sci. Technol.*, 36; 8: 653–660.

- [8] Kang, K., Zhao, L., Zhou, J., Liu, S., An, Q., (2013). A 128-channel high precision time measurement module, *Metrol. Meas. Syst.*, Vol. XX, No. 2, 275–286.
- [9] Song, J., An, Q., Liu, S., (2006). A High-Resolution Time-to-Digital Converter Implemented in Field-Programmable-Gate-Arrays, *IEEE Transactions on Nuclear Science*, VOL. 53, NO. 1.
- [10] Wang, H., Zhang, M., Liu, J., (2011). High-Resolution Short Time Interval Measurement System Implemented in a Single Fpga Chip. *Chinese Sci Bull*, 56:1285–1290, doi: 10.1007/s11434-011-4421-3
- [11] Ugur, C., Bayer, E., Kurz, N., Traxler, M., (2012). A 16 Channel High Resolution (<11 Ps RMS) Time-To-Digital Converter in a Field Programmable Gate Array, *Topical workshop on electronics for particle physics, Vienna, Austria*.
- [12] Mathworks, (2011). *MATLAB Reference Guide*. The Math Works Inc.
- [13] Kalisz, J., (2004). Review of Methods for Time Interval Measurements with Picosecond Resolution, *Metrologia*, 41: 17–32.
- [14] Zieliński, M., (2009). Review Of Single-Stage Time-Interval Measurement Modules Implemented in FPGA Devices, *Metrol. Meas. Syst.*, 16; 4: 641–648.
- [15] Henzler, S., (2010). *Time-to-Digital Converters*, Springer.
- [16] Carbone, P., Kiaei, S., Xu, F., (2014). *Design, Modelling and Testing of Data Converters*, Springer.
- [17] *NIOS II Software Developer's Handbook Version 11.1*, (2011). ALTERA Corporation.
- [18] Zieliński, M., Kowalski, M., Frankowski, R., Chaberski, C., Grzelak, S., Wydźgowski, L., (2009). Accumulated Jitter Measurement of Standard Clock Oscillators, *Metrol. Meas. Syst.*, Vol. XVI, No. 2, 259–266.
- [19] Artyukh, Y., Boole, E., (2011). Jitter Measurement on the Basis of High-Precision Event Timer, *Metrol. Meas. Syst.*, Vol. XVIII, No. 3, 453–460.
- [20] *STRATIX III DSP Development Kit Reference Manual*, (2008). ALTERA Corporation.
- [21] *QUARTUS II Handbook Version 11.1*, (2011). ALTERA Corporation.
- [22] *SOPC Builder User Guide*, (2010). ALTERA Corporation.
- [23] Arkani, M., Khalafi, H., Vosoughi, N., (2013). A Flexible Multichannel Digital Random Pulse Generator Based on FPGA, *World Journal of Nuclear Science and Technology*, Vol. 3 No. 4, 109–116. doi: 10.4236/wjnst.2013.34019.
- [24] Arkani, M., Khalafi, H., Arkani, M., (2013). Efficient dead time correction of G-M counters using feed forward artificial neural network, *Nukleinika*, 58(2): 317–321.
- [25] Arkani, M., Khalafi, H., Arkani, M., (2013). An Improved Formula for Dead Time Correction of GM Detectors, *Nukleinika*, 58(4): 533–536.
- [26] Knoll, G.F., (1999). *Radiation Detection and Measurement*, John Wiley & Sons, Inc.